https://doi.org/10.5194/essd-2025-692
Preprint. Discussion started: 27 November 2025

Lagoon temperature and hydrodynamics of Reao Atoll (Tuamotu Archipelago, French Polynesia) before and during the 2024 El-Niño Marine Heatwave

Esther Ladet[1], Carla Chevillard[1], Romain Le Gendre[2,3], Thomas Trophime[4], Sébastien Petton[5], Simon Van Wynsberge[1]

[1]Ifremer, IRD, ILM, UPF, UMR 241 SECOPOL, Vairao, 98725, Tahiti, French Polynesia
[2]Ifremer, UMR 9220 ENTROPIE (Ifremer, IRD, Univ. Réunion, Univ. Nouvelle-Calédonie, CNRS), BP 32078, 98897 Nouméa CEDEX, New Caledonia
[3]Université de Toulouse, LEGOS (CNES/CNRS/IRD/UT3), Nouméa, Nouvelle-Calédonie, France
[4]Direction des Ressources Marines, Papeete, 98713, Tahiti, French Polynesia
[5]Ifremer, Univ. Brest, CNRS, IRD, LEMAR, F-29840, Argenton, France

Correspondence to: Simon Van Wynsberge (simon.van.wynsberge@ifremer.fr) and Romain Le Gendre (romain.le.gendre@ifremer.fr)

Abstract. In French Polynesia, semi-closed atolls of the eastern Tuamotu Archipelago are home to fisheries and mariculture activities based on giant clam resources. These activities are increasingly vulnerable to global warming, as evidenced by the mass bleaching event observed in Reao atoll in March 2024, triggered by the most intense and prolonged Marine Heatwave (MHW) ever recorded in this lagoon. The GAIA project (manaGement strAtegy evaluatIon for small-scale fisheries in Atoll lagoons) was launched to address this issue and aimed to explore the sustainability of giant clam fisheries under climate change, with a particular focus on processes driving thermal exposure during MHWs. To achieve this, spatial and temporal temperature fluctuations, lagoon circulation, and water exchange dynamics between ocean and lagoon across the atoll rim were monitored using moored autonomous oceanographic sensors. A total of 6 monitoring periods took place between December 2016 and May 2025, with the most extensive instrumentation covering the entire February-March 2024 MHW event. The strength of these observations lies not only in their coverage of a unique and poorly sampled ecosystem, but also in their comprehensive documentation of an exceptional MHW event, from its onset and peak to its dissipation, providing an unprecedented record of the full life cycle of a major thermal anomaly in a tropical semi-closed atoll lagoon. This dataset also supports future modelling efforts to simulate temperature dynamics and identify thermal refugia in atoll lagoons under changing climate scenarios. All data were post-processed, quality-controlled, and formatted into interoperable NetCDF files. The full dataset is openly accessible through the SEANOE marine data platform: https://doi.org/10.17882/105885 (Le Gendre et al., 2025a).

https://doi.org/10.5194/essd-2025-692
Preprint. Discussion started: 27 November 2025

1 Introduction

Semi-closed lagoons are widespread in the eastern Tuamotu Archipelago, French Polynesia, yet they represent unique hydrodynamic systems primarily shaped to their geomorphological configuration (Rougerie, 1995; Andréfouët and Paul, 2023). Unlike previously documented lagoons (Bruyère et al., 2023), semi-closed atolls are characterized by the absence of reef pass, with shallow channels crossing the rim ("*hoa*") found only on one side of the atoll. In semi-open atolls (those including passes), water inflows through the *hoa* and the reef pass are mainly driven by tide and oceanic incident waves, and outflow of excess water is drained mostly through the pass (Dumas et al., 2012; Aucan et al., 2021). However, for semi-closed atolls, hydrodynamic behaviour can differ markedly and these lagoons may become temporarily isolated from the ocean (Van Wynsberge, 2016). Water exchange from the ocean into these lagoons occurs only when offshore wave energy reaches a threshold sufficient to drive oceanic water across the atoll rim, through *hoa*. This threshold is likely modulated by tidal range and external sea level anomalies. During periods of low swell, or when swell direction is not congruent with the open rim's orientation, exchanges become minimal or even interrupted, causing lagoon water levels to drop significantly due to enhanced evaporation — a condition locally referred to as *ranoa*. Consequently, these atolls can experience long periods of highly restricted water renewal, during which they are particularly sensitive to atmospheric conditions and heat fluxes (Andréfouët et al., 2022). While semi-closed lagoons can become temporarily isolated from the ocean, they are also highly vulnerable to the opposite extreme. Extreme surges generated by prolonged, powerful incident swells, and associated land flooding (Storlazzi et al., 2018; Andréfouët et al., 2023), are exacerbated in semi-closed lagoons, due to the lack of a pass to drain excess water. Monitoring lagoon water levels during such events provides key insights into lagoon responses to extreme hydrodynamic forcing.

When these lagoons temporarily behave as closed systems, thermal stress imputed to marine organisms can be aggravated (Van Wynsberge et al., 2017), sometimes leading to mass mortalities (Van Wynsberge & Andréfouët, 2017; Andréfouët et al., 2022). These dynamics have important consequences for giant clam populations (*Tridacna maxima*), a species of ecological, economic, and cultural significance across Indo-Pacific coral reef ecosystems (Neo et al., 2015; Mies et al., 2017). In the semi-closed lagoons of the Tuamotu Archipelago, giant clams can form dense aggregations that support local fisheries and mariculture (Gilbert et al., 2005; Remoissenet & Wabnitz, 2012; Van Wynsberge et al., 2016; Andréfouët et al., 2025). However, their symbiotic relationship with Symbiodiniaceae makes them vulnerable to thermal stress (Teaniniuraitemoana et al., 2025), raising concerns under climate change scenarios. In particular, recurrent mass bleaching events linked to El Niño-driven marine heatwaves (MHWs) have impacted *T. maxima* stocks, with implications for both the fishery and the aquarium trade (Andréfouët et al., 2018; Van Wynsberge et al., submitted). In this context, characterizing the spatial and temporal variability of local temperature regimes, and understanding their drivers is essential, notably with intensifying climate extremes.

https://doi.org/10.5194/essd-2025-692
Preprint. Discussion started: 27 November 2025

This study presents a rare and comprehensive dataset of multi-year monitoring of temperature and sea level inside the semi-closed lagoon of Reao. Moreover, a more extensive instrumentation setup enabled enhanced lagoon sampling before and during the most prolonged and intense MHW ever recorded locally (Van Wynsberge et al., submitted), which was associated with the 2024 strong mixed El Niño (Pagli et al., 2025). The sampling strategy captured both horizontal and vertical temperature variability via moored sensors at relevant lagoon sites and depths, as well as through vertical profiles (from CTD casts). Continuous measurements of lagoon level, circulation, and ocean-lagoon exchanges have also been acquired during the austral summer 2023-2024. Instrumenting the diverse geomorphological strata, including *hoa*, the inner reef slope, lagoon patch reefs, and deep lagoon areas, provides a system-wide view of the hydrodynamic variability and processes within the lagoon before and during such an extreme event, and sheds light on the hydrodynamic and atmospheric forcings that control intensity and duration of MHW inside semi-closed atoll lagoons. After a presentation of the study site in Section 2, the instruments and deployment methods are described in Section 3, followed by the sampling strategy (Section 4) and the data processing and quality control procedures in Section 5. Finally, illustrative observations of this semi-closed atoll dynamics are shown in Section 6.

2 Study site

Reao Atoll (18.45°S–18.6°S; 136.25°W–136.5°W) located at the eastern end of the Tuamotu archipelago (French Polynesia ; Fig.1.B) is a shallow atoll known for harboring one of the world's highest densities of the giant clam *Tridacna Maxima* (Van Wynsberge and Andréfouët, 2017). Its population (329 inhabitants according to the 2022 census) lives mainly in the village located on the northwestern part of the atoll, and largely rely on giant clam resources (for flesh or aquarium trade). Reao is classified as a semi-closed atoll, with a fully emerged rim in its north-eastern part, and a southern rim segmented by an alternation of low-lying sandy islets, locally known as *motu*, and numerous shallow natural channels (*hoa*), which allow limited water exchange between the lagoon and the open ocean (Fig. 1). Lagoon aperture (defined as the ratio of the sum of the widths of all functional channels to the atoll perimeter) ranges from 1% to 13% depending on water level (Andréfouët et al., 2022). The numerous *hoa* vary greatly in shape (see Fig.1.C and Appendix A, Fig. A2), width and depth, but the most active ones are located in the central part of the southern rim (Tarahaero; Fig. 1C). The atoll rim delimits a lagoon of 38.33 km² with an average depth of 16 m (maximum depth: 32 m). Elongated along a northwest–southeast axis, the lagoon comprises three distinct basins, the northwestern (NW), the intermediate, and the southeastern (SE) basins, which progressively widen and deepen from north to south (Fig. 1.A; Quéré et al., 2025). Overall, the three basins exhibit a bowl-shaped morphology, with shallower margins surrounding deeper central areas.

Four distinct daily wind regimes (WRs) affect the area (Dutheil et al., 2020). The dominant regime (WR1) corresponds to a persistent trade-wind pattern, characterized by a strong homogeneous east-southeast flow (WR1, 6.3 m.s-1, ~ 100°). Two additional easterly regimes (WR2 and WR3), differ mainly in intensity (resp. 4.4 and 3.9 m.s-1) or orientation (resp. 107.5° and 75.3°). A fourth regime (WR4) associated with weaker north-easterly winds (64.9°, 3 m.s-1) predominates during the

https://doi.org/10.5194/essd-2025-692
Preprint. Discussion started: 27 November 2025

austral summer and disappears in austral winter (in opposition to WR1). Regarding the wave climate, the region is dominated in austral winter by high-amplitude, long period southwesterly incoming swells (R1, Hs = 2.5m, Tp = 13.4s and coming from 190°). During austral summer, northwesterly swells (R3) of lower amplitude (235°, 2 m) but similar periods prevail; yet Reao Atoll remains largely unaffected due to its impermeable northern rim. South-southeast wind waves (R2) generated by tradewinds also occur year-round with a peak in May-July (Dutheil et al., 2021).

https://doi.org/10.5194/essd-2025-692
Preprint. Discussion started: 27 November 2025

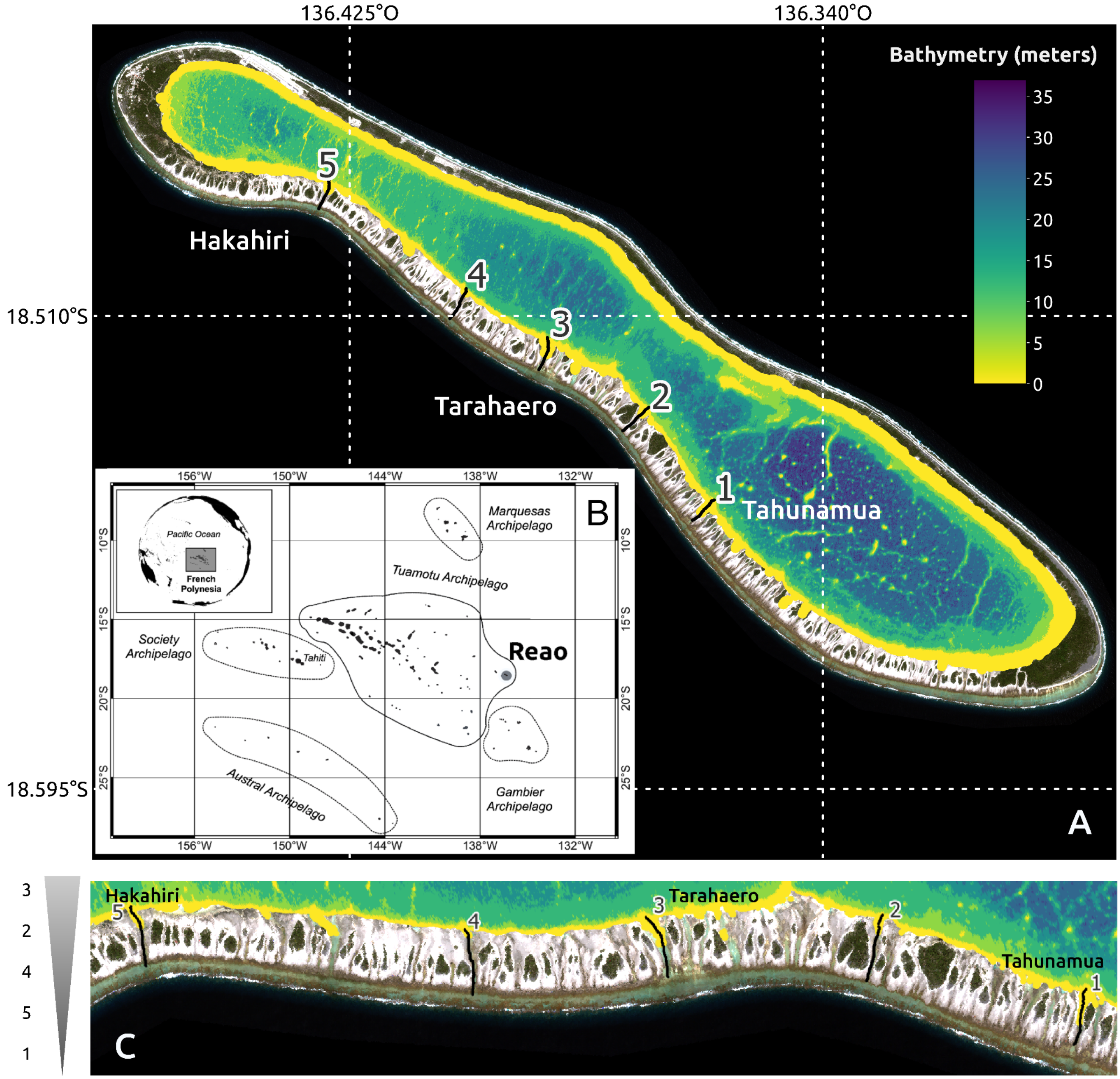

Figure 1: A) Satellite-derived bathymetry of Reao retrieved from Sentinel-2 imagery (Copernicus Sentinel-2, 2021; Quéré et al., 2025a, 2025b) using the method of Amrari et al. (2021). B) Location of Reao within the French Polynesian archipelagos (Credit: Oriane Bruyère). C) Numbers indicate the main hoa (numbered from south to north). This panel shows the *hoa* according to their width and minimum depth, with *hoa* n°3 (locally called Tarahaero), located along the central section of the southern rim, being the most open, and *hoa* n°1 (locally called Tahunamua), located along the southern section of the southern rim, being the least open (Quéré et al., 2025b).

https://doi.org/10.5194/essd-2025-692
Preprint. Discussion started: 27 November 2025

3 Instruments, methods and deployments

Various physical oceanographic instruments were deployed during the GAIA project to monitor thermal variability, ocean-lagon exchanges and lagoon dynamics. These included moored compact loggers dedicated to temperature and pressure, as well as different types of current meters (point-measurement devices and vertical profilers). During each field campaign, conductivity–temperature–depth (CTD) profiles were performed throughout the lagoon allowing to capture the vertical structure of the water column. All profiles were performed manually from a boat. A detailed list of all instruments, including manufacturer, model, raw and processed parameters, deployment location, logging frequency, and deployment period, is provided in Appendix A (Table A1).

All moorings were deployed by scuba diving and adapted to the seabed habitats and deployment sites to ensure stability during highly energetic events. Mooring supports were constructed from a variety of materials, including concrete blocks, steel bars, and equipped with sacrificial anodes to prevent corrosion or electrolysis damage (see Fig. 2). To minimize biological fouling, Acoustic Doppler Current Profilers (ADCPs) were coated with cayenne pepper and grease and then wrapped with electrical tape, while smaller compact loggers were enclosed in perforated plastic cylinders (see Fig. 2a) to allow water circulation while providing protection against biofouling and mechanical damage. Mooring depths were measured using a dive computer (for sensors without pressure) or derived from the mean water depth over the whole deployment period (for sensors equipped with pressure). All moored instruments were autonomous, containing internal batteries and memory to support long-term deployment.

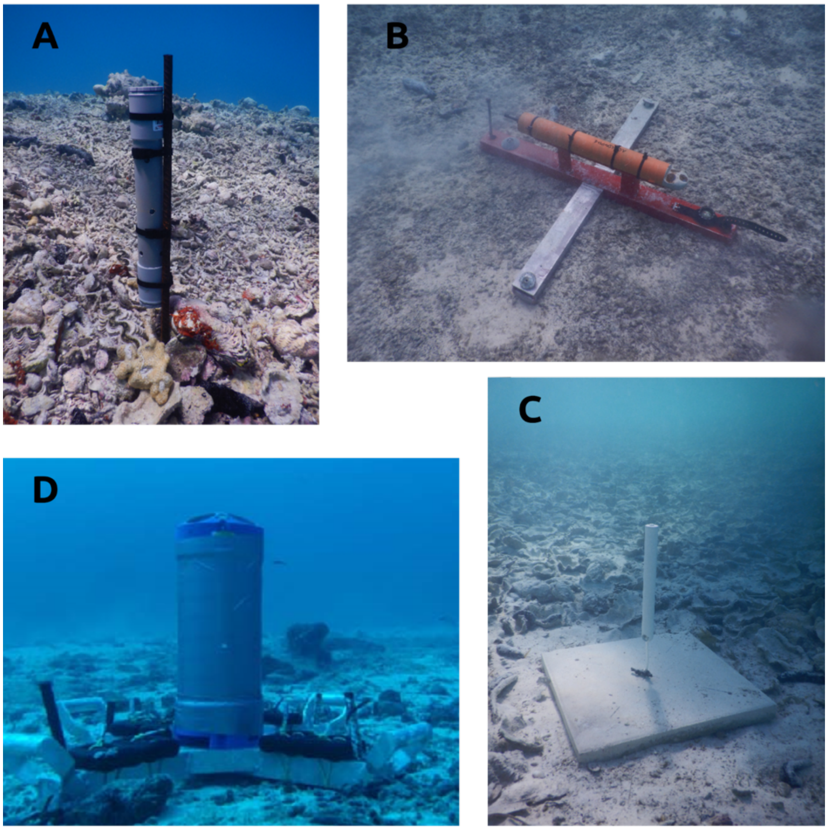

Figure 2: Photos of the moored sensors deployed in Reao Lagoon: RBRduet/SBE56 (A), Aquadopp (B), Lowell TCM-4 (C), ADCP Sentinel (D). Photo credit : Simon Van Wynsberge.

3.1 Compact loggers: Temperature and Pressure

Three types of compact loggers were used across the various deployments to monitor either temperature or temperature and pressure. The first set of sensors included 15 SBE56 loggers (Sea-Bird Scientific Inc.: https://www.seabird.com/sbe-56-temperature-sensor/product?id=54627897760 ; last access: 7 November 2025). All SBE56 deployed during the GAIA project were new and directly came from the manufacturer, thus, given the specifications of these high-accuracy sensors, the data are delivered with a maximum uncertainty of ±0.01°C. The typical sampling period was 1 min (Appendix A - Table A1). The second set of compact loggers consisted of two RBR Ltd. models, namely TWR-2050 and RBduet T.D (https://www.bodc.ac.uk/data/documents/nodb/pdf/rbr_tide_wave_07apr2011.pdf ; https://rbr-global.com/products/compact-loggers/rbrduet-td/ ; last access : 7 November 2025). The TWR-2050, a 10 dbar range sensor, was deployed during the first deployment period only (2016–2017) and sampled water level and temperature every 30min. Its maximum uncertainty regarding pressure was estimated around 0.5% of full scale (± 5 cm) and ±0.01°C for temperature. All RBRduet Temperature-Depth sensors (RBR Ltd) were returned from the manufacturer recalibration just before the start of

https://doi.org/10.5194/essd-2025-692
Preprint. Discussion started: 27 November 2025

sampling. Based on their specifications, a maximum uncertainty of less than 1 cm in level and 0.004 °C in temperature. can be expected. Typical sampling periods were set to 1Hz..

3.2 Current meters

Two types of current meters, namely drag-tilt current meters and Acoustic Doppler Current Profilers (ADCPs), were installed in Reao lagoon to monitor the austral summer 2023-2024. The Lowell TCM-4 drag-tilt current meter is an autonomous, low-cost instrument that estimates current velocity and direction from sensor tilt, while also recording temperature (https://lowellinstruments.com/tilt-current-meters/tcm-4-tilt-current-meter/;last access : 7 November 2025). Five TCM4 were used during the GAIA project sampling. All these sensors were new at the beginning of their deployment (Leg 4) thus providing a maximum uncertainty of 5 cm.s-1 in current speed, 5° in direction and 0.1°C in temperature. Their typical sampling period was set to 1 min. ADCP Sentinel V series (Teledyne RD Instruments; https://www.teledynemarine.com/en-us/products/SiteAssets/RD%20Instruments/Sentinel_V_combined.pdf; last access : 7 November 2025) provide current profiling over the water column in coastal environments. Two models were deployed: a Sentinel V20 and two Sentinel V50. The Sentinel V-series provides three-dimensional velocity measurements as well as bottom temperature and pressure observations. The northern basin was equipped with a V20 (1000 kHz), and two Sentinel V50 (500 kHz) were deployed in the intermediate and southern basins. Globally, bursts were programmed every 20 min, with 90 pings per burst (1 s ping interval). Cell sizes were set to 0.5 m for the V20 and 1 m for the V50 and the first measured cell above the blanking zone was at 1.01 m (resp 2.22 m) for V20 (resp. V50).Both awaited standard deviation for current speed was 0.74 cm/s. The Aquadopp (Nortek) is an acoustic current meter used to measure current speed, direction, temperature, and pressure in shallow environments (https://www.nortekgroup.com/products/aquadopp-profiler2-1-mhz; last access: 7 November 2025). During the GAIA project the two models were 2MHz side-looking heads deployed in *hoa.* Burst sampling period was programmed to 20 min, with a cell size of 0.2 m,and a blanking distance of 0.2 m leading to precision of horizontal velocity observations of 2.3 cm/s.

3.3 CTD Profiles

The CTD (Conductivity Temperature Depth) profiles were obtained using a Sea-Bird 19Plus V2 SeaCAT Profiler CTD (Sea-Bird Scientific ; https://www.seabird.com/sbe-19plus-v2-seacat-profiler-ctd/product?id=60761421596; last access: 7 November 2025), which measures conductivity, temperature, and pressure at a sampling frequency up to 4Hz. The SBE19Plus V2 provides high-resolution and highly reliable measurements. Its last maintenance and manufacturer recalibration date back to 2022, which ensures high measurement accuracy (maximum uncertainty lower than that of moored loggers).

https://doi.org/10.5194/essd-2025-692
Preprint. Discussion started: 27 November 2025

4 Sampling strategy

The sampling design implemented under the GAIA project evolved throughout its duration to progressively address both thermal and sea-level vulnerabilities of semi-closed atoll lagoons. Prior to the GAIA project, an early historical 7-month deployment of a temperature and pressure sensor was performed (Leg 1, Station T1 from 17 December 2016 to 29 June 2017) and helped design the project sampling.

At the early stage of the project, a first temperature logger was deployed in June 2021 (Figure 3; Figure A1 - Station T2 - Leg 2 to 6) during a first fieldwork dedicated to giant clam stock assessment and health monitoring. The initial objective was to begin a continuous interannual record of lagoon temperature, providing a baseline reference and ensuring long-term monitoring of Reao's lagoon temperature observations that are included in the SNO ReefTEMPS network (Le Gendre et al., 2025). Following the acquisition of additional instruments within the GAIA project, the spatial coverage of the monitoring network was substantially increased, allowing a refined characterization of thermal dynamics across key lagoon sectors.

Subsequent field campaigns (Legs 4 to 6; from June 2023 to May 2025) implemented a more advanced experimental design using up to 18 moored instruments, aimed at better understanding of the hydrodynamic functioning of the lagoon, including ocean–lagoon exchanges, lagoonal circulation, and spatial and vertical temperature dynamics through multi-depth moorings.

4.1 Ocean-lagoon exchanges and lagoon level

One of the key objectives of the GAIA sampling strategy was to better understand the mechanisms governing water exchanges between the ocean and the lagoon through the *hoa*. The selection of *hoa* to be instrumented (see Fig 1.B and Fig A.3) was made following extensive field reconnaissance during the beginning of Leg 4, combining direct observations of their functioning with geomorphological characteristics (depth, width, orientation) and local knowledge of their hydrodynamic behaviour.

The monitoring design aimed to cover *hoa* distributed across different sectors of the reef rim and representative of the three main lagoonal basins (northern, intermediate, and southern). To this end, five Lowell TCM-4 drag–tilt current meters were deployed at stations L1 to L5 during Leg 4 (Fig 3.A). These autonomous instruments recorded current speed and direction, together with temperature, providing insights into the temporal variability of ocean–lagoon fluxes.

During Leg 5, the setup was complemented by two Nortek Aquadopp current profilers deployed at stations A1 and A2, corresponding respectively to the TCM-4 sites L3 and L1. These profilers allowed finer characterization of velocity structure across selected *hoa*, while also documenting temperature and sea-level variability.

Lagoon water level variability was monitored during several legs of the GAIA project. The first observations were obtained during Leg 1 using an RBR TWR-2050 sensor deployed at station T1, followed by an RBRduet T.D logger installed at station

https://doi.org/10.5194/essd-2025-692
Preprint. Discussion started: 27 November 2025

T11 from legs 3 to 5. These long-term pressure records were specifically designed to document lagoon-level variability under varying environmental conditions, notably the influence of incident oceanic swells and sea-level anomalies. During Leg 5, additional sea level measurements were available from pressure records provided by the Aquadopp profilers positioned in the *hoa* (stations A1 and A2, Fig 3.A), as well as from the three ADCP Sentinel V instruments deployed within the lagoon.

4.2 Lagoonal circulation

The three ADCPs (stations B1 to B3, Fig. 3.A) were strategically located to capture current profiles from the surface to the bottom in each of the three main lagoonal basins and broadly positioned along the atoll's main axis. This configuration enabled the characterization of internal lagoon circulation patterns and their response to hydrodynamic forcing, including wind stress and ocean–lagoon exchange processes. Combined, these complementary observations provide a comprehensive view of lagoon-level variability and circulation dynamics under contrasting meteorological and oceanic conditions.

Building on this carefully designed sampling strategy, the following section describes the procedures applied to process, validate, and standardize the collected data to produce a high-quality, interoperable dataset.

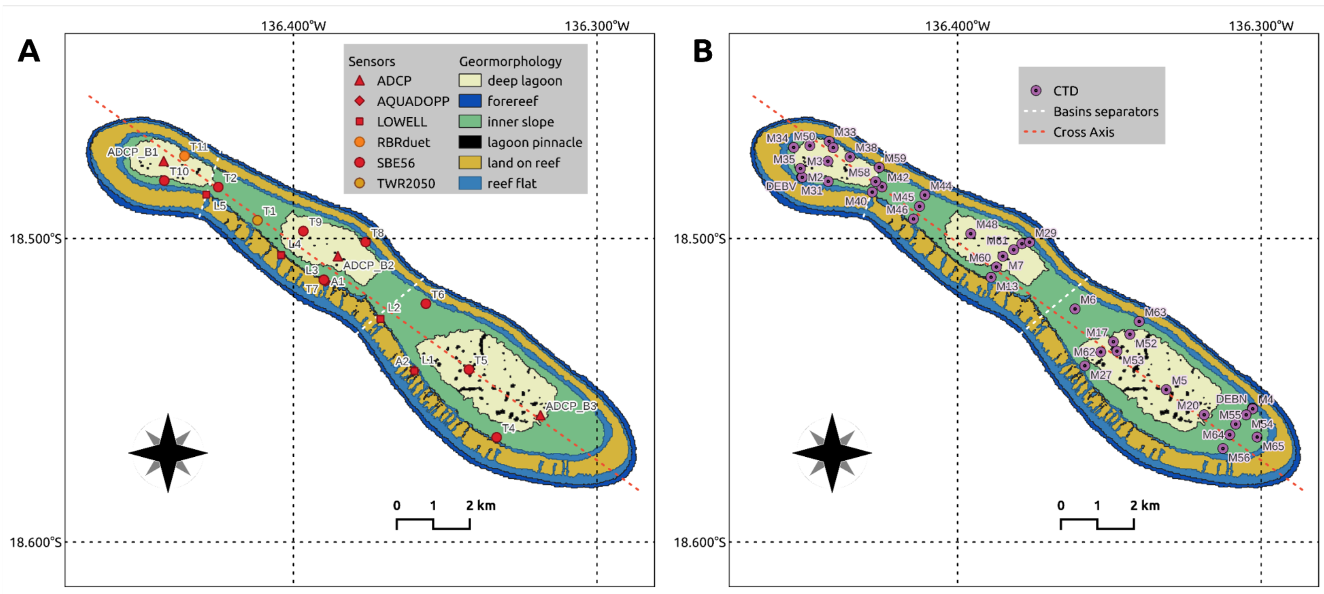

Figure 3: Deployment scheme of moored loggers (A) and Conductivity, Temperature, Depth (CTD) vertical profiles (B) performed at Reao. Background colors on the map refer to reef geomorphology, from Andrefouet et al. (2012).

https://doi.org/10.5194/essd-2025-692
Preprint. Discussion started: 27 November 2025

4.3 Spatial and vertical temperature variability

To characterize spatial temperature variability, a network of moored SBE56 loggers was deployed across different lagoonal and rim environments (stations T1 to T11; Fig. 3A), covering the northern, intermediate, and southern basins for periods ranging from 6 to 34 months, depending on the sensor (Table A1). Temperature loggers were placed in the 1-3 m depth range where giant clams are preferentially found. However, two lagoon patch reefs (stations T4 and T10) were instrumented with additional loggers placed deeper (4.5 and 7 m depth) to set up vertical temperature sensor arrays during Leg 5 (6 months), which includes the February-March 2024 MHW event. Vertical stratification of temperature was further characterized with CTD vertical profiles performed in June 2023 (2–13 June), October 2023 (13–18 October), and during the 2024 MHW, on 29 March. CTD profiles were spatially distributed to cover the Northern basin, where mariculture activities take place, and along five radials crossing the lagoon widthwise according to a distance gradient to the open rim (Fig. 3B). Because CTD profiles measured both temperature and salinity, they also provided insights on water renewal, basin characteristics and vertical stability of water masses.

5 Data processing and quality controls

The processing and quality control procedures applied to this dataset build upon extensive prior experience in lagoon monitoring. To ensure both data quality and interoperability—using consistent file formats and instrument types—the same methods for processing, formatting, and quality control as described in previous studies were applied (Bruyère et al., 2022; Bruyère et al., 2023a; Bruyère et al., 2023b).

Raw data were retrieved from each instrument using the manufacturer's software and saved on a secure network drive. Each file was renamed following a standardized nomenclature containing key deployment information: Atollname_Station_Instrument-Model_SerialNumber_Depth_LegNumber.filetype. Data were then visually inspected to identify and remove bad records (e.g., out-of-water readings, spikes, or outliers) and to determine the exact start and end times of valid observations (based on our field notes and confirmed using pressure and temperature plots).

Data was subsequently converted into formats suitable for processing with Python 3 routines, typically ASCII or MATLAB files, processed as needed and finally exported as NetCDF files. Each NetCDF file includes temperature, pressure, current, or other relevant variables, together with comprehensive metadata such as deployment dates, time reference (expressed in UTC for all instruments), geospatial coordinates, depth, instrument model and serial number, project and investigator information, processing history, and comments to ensure reusability.

Specific processing steps were applied depending on instrument type:

https://doi.org/10.5194/essd-2025-692
Preprint. Discussion started: 27 November 2025

- RBRduet T.D sensors: pressure data were corrected for a constant atmospheric pressure (101 325 Pa) to minimize weather-related variability. No precise vertical referencing by DGPS was possible due to deployment conditions. Water level was calculated relative to the long-term mean depth. For wave analysis, pressure records were filtered using a Fourier transform to obtain a pressure spectrum (3–25 s period), and linear wave theory with a homogenous cut-off frequency (0.33) was applied to compute wave parameters. Two output files were generated: one with 1-minute resolution for temperature and water level, and another with 1-hour resolution containing derived wave parameters.
- Current meters (ADCPs, Aquadopps, and Lowell TCM-4): vertical profiles near the surface were removed to avoid contamination from acoustic reflections or noise. Data were converted to consistent coordinate systems (East - North - Up), and orientation conventions were harmonized with oceanographic standards. Temporal and vertical resolutions were retained according to deployment settings.
- Compact loggers (SBE56): temperature data were generally retained at the original sampling frequency without additional processing.
- CTD casts: standard processing using SeatermV2 software was applied, including conversion to .cnv, low-pass filtering, alignment of sensors, derivation of secondary parameters, and vertical bin averaging (0.5 m).

After processing, all datasets were visually inspected using Ferret and NetCDF tools to certify the quality of the time series and detect eventual anomalies. Any remaining outliers or unusual observations were flagged in the NetCDF global attributes. Metadata were systematically checked to verify the completeness and correctness of global and variables' attributes. These procedures ensure a high-quality, standardized, and interoperable dataset suitable for scientific analysis and long-term monitoring of lagoon dynamics.

6 Overview of observations

6.1 Ocean-lagoon exchanges and lagoon level

Figure 4 shows the temporal variability of ocean–lagoon exchanges over a 5-day subset for the five instrumented *hoa*, highlighting differences in exchange intensity and dynamics among sites, together with lagoon-level variations at station T11. This period was selected as it encompasses a short but energetic incident swell event (from 22 to 24 October 2023, Fig. 4). Globally, a good synchronicity in the patterns of inflow/outflow between the five instrumented *hoa* was observed (based on velocity projections along each *hoa*'s main axis). For all of them, inflows and outflows followed the offshore tidal trend, with inflows dominating between mid-flood and mid-ebb, and vice versa. During this period, currents in the *hoa* reached values exceeding 1 m s^{-1} (station L2 at the peak of the event). It is noteworthy that during this swell episode, the most active *hoa*—i.e., those exhibiting the strongest inflowing currents—were the central ones along the southern rim (L3, A1, and L2). At the peak of the event, all *hoa* were almost exclusively inflowing for about two consecutive tidal cycles. Similarly, lagoon drainage

https://doi.org/10.5194/essd-2025-692
Preprint. Discussion started: 27 November 2025

appears to occur mainly through the central *hoa* (L4, L3, A1 and L2), which exhibit longer durations and higher intensities of outgoing currents compared to those located at the northern and southern extremities. Figure 4 also demonstrates good congruence between Aquadopp and Lowell-TMC4 records, since similar currents speed and direction were found for instruments A1 and L3, which were positioned a few meters apart, in the same *hoa*. Finally, the lagoon water level shows a faster filling than drainage phase, with an increase of more than 30 cm in less than 24 hours.

The inconsistent behaviour of A2 currents with other currents at the beginning of the time series of Figure 4 might be explained by the location of the sensor in a *hoa* with a coarser complex bathymetry (see locations of sensors in the different *hoa* in Appendix A2). Such location appears to have an impact on A2 currents when currents are rather low in other *hoa*. When currents increase due to swell events, a better coherence is observed with A2.

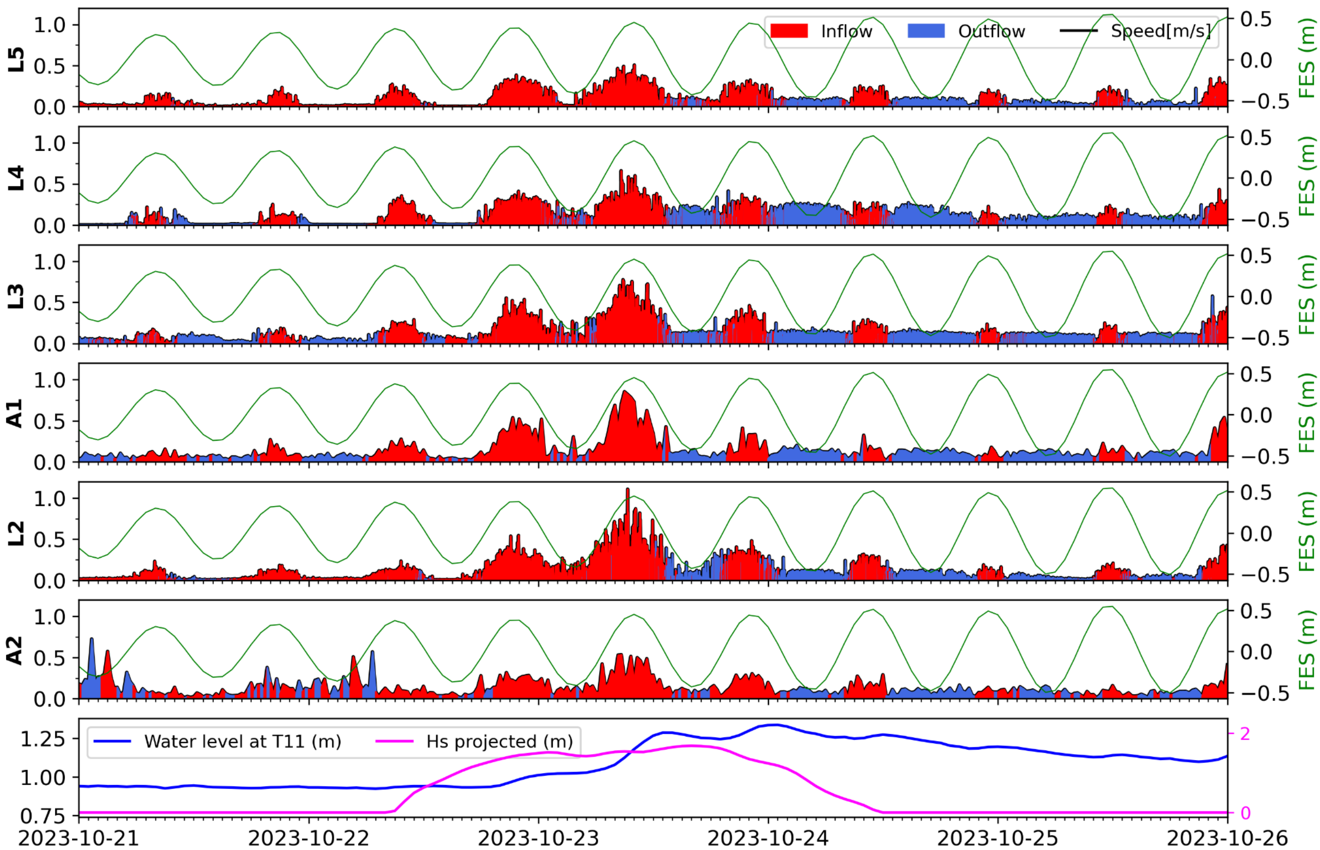

Figure 4: Current speed and direction (inflow in red, outflow in blue) recorded by Lowell-TCM4 L2, L3, L4, L5) and Aquadopp (A1, A2) in *hoa*. Instruments A1 and L3 were positioned a few meters apart within the same *hoa*. The ocean tide (reconstructed from FES 2012 global tide solution) is shown as solid green lines in each panel. The bottom panel displays the lagoon water level at T11 (blue) and ERA5 projected significant wave height (pink, Hs at 18.75°S, 136.6°W) projected onto the direction normal to the southern rim (210°).

https://doi.org/10.5194/essd-2025-692
Preprint. Discussion started: 27 November 2025

6.2 Lagoonal circulation

Globally, currents display very low values (average velocities around 2.5 cm/s for the three instruments, and for all cells across the profiles). Depth-averaged currents generally exhibit relatively stronger currents in the northern basin than in the intermediate and southern basins (up to 0.1, 0.07, 0.06 m/s maximum current velocities respectively for B1, B2 and B3). Fig. 5 is a 7-day example (25 November–1 December 2023) of circulation captured in the three current profilers (stations B1, B2 and B3) deployed in the lagoon, associated with the wind induced slope. Winds and currents are both projected along Reao's main axis and slope is computed as the difference in depth anomalies between B1 and B3. At the beginning and at the end of this sequence, positive projected wind values indicate trade winds (blowing from East-Southeast). They induce a slight sea surface slope of around 2cm at maximum during the displayed period. Globally, Fig. 5 shows vertically sheared currents across the three instruments, with surface currents flowing to the northwest (note that the first few meters were discarded to avoid "contaminated" values) and the deeper currents flowing to the southeast. It is particularly visible at station B3 during the first (and last) two days (25-26 November). These patterns suggest the existence of overturning circulations as described in Dumas et al. (2012) for the case of Ahe atoll. At this stage, we cannot determine whether these circulation cells are specific to each basin, but further hydrodynamics modeling will provide insights about these patterns. Finally, the effect of a wind reversal (with a northwest wind burst around 28 November) appears on Fig. 5 with the establishment of the inverse patterns of circulation.

https://doi.org/10.5194/essd-2025-692
Preprint. Discussion started: 27 November 2025

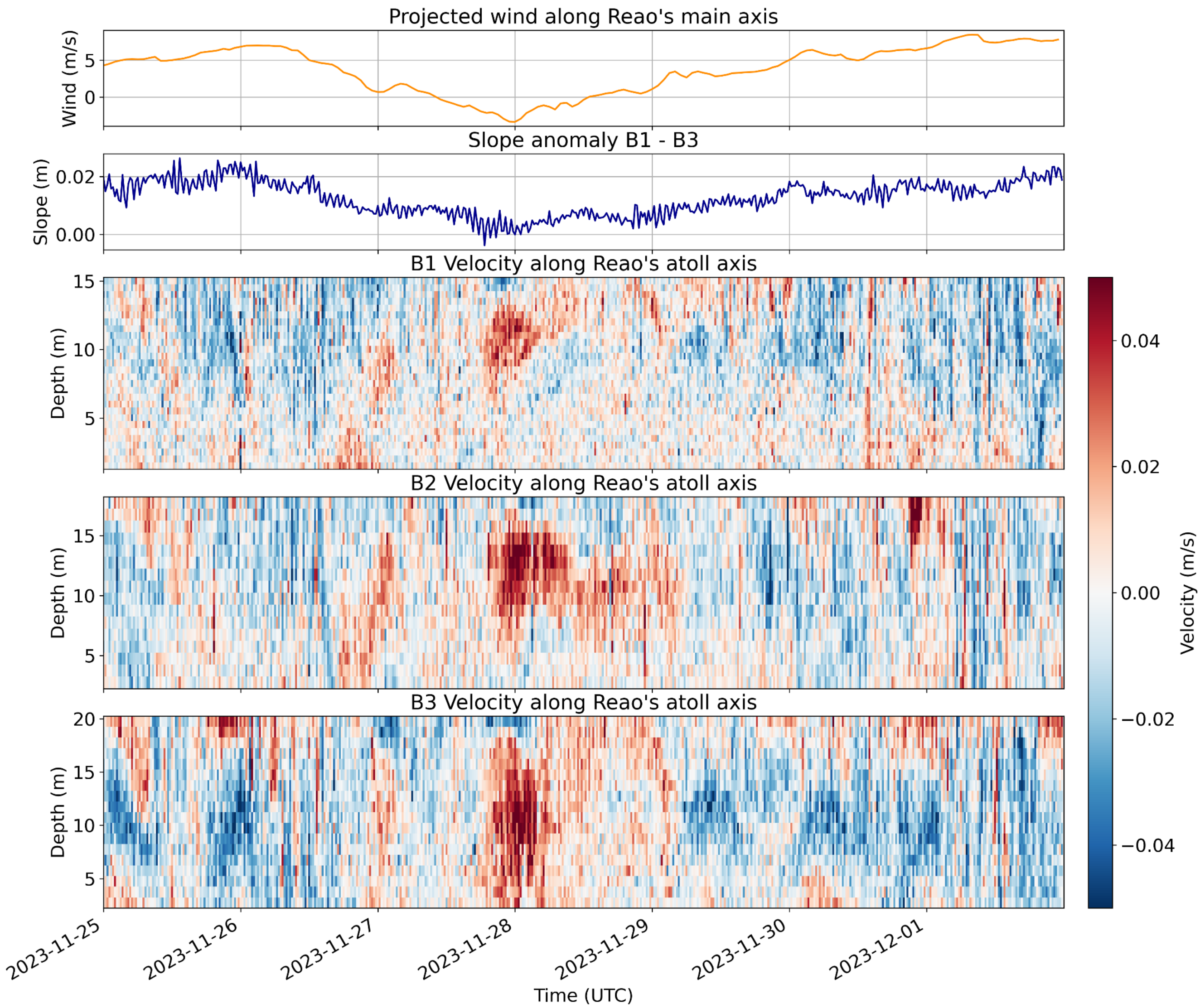

Figure 5: From top to bottom: ERA5 winds (18.5°S, 136.5°W) projected onto Reao's major axis (positive values indicate winds blowing from southeast toward northwest); sea surface slope between ADCP B1 and ADCP B3 (positive values indicate higher water level at B1); and profiles of projected current velocities along Reao's main axis (positive values indicate currents flowing toward the northwest).

6.3 Observed thermal patterns with a focus on the 2024 MHW event

The temperature time series allowed us to characterize the seasonal trend of temperature in Reao's lagoon. As already described in other atoll lagoons (Van Wynsberge et al., 2017), lagoon temperature covered a broader range of values than ocean SST (here ERA5 SST at 18.75°S, 136.6°W), with higher lagoon temperature than ocean SST in austral summer, and vice versa in

https://doi.org/10.5194/essd-2025-692
Preprint. Discussion started: 27 November 2025

austral winter (Fig. 6.A). During the GAIA sampling, the Reao lagoon experienced four distinct MHWs: three short category I events and one category III event (Van Wynsberge et al., in revision). The category I events spanned 13 days (25 March–7 April 2023), 5 days (24–29 April 2023), and 6 days (3–9 January 2024).

The category III event , which occurred from 19 February to 30 March 2024, persisted for 40 days.. During this period, both oceanic SST and lagoon temperature increased, but the lagoon warmed more rapidly, remaining on average ~1.39 °C above SST, reaching a maximum difference of ~1.97 °C. Only weak vertical temperature gradients were observed between 1 m, 4 m, and 7 m depths at station T10, although the diurnal amplitude was more pronounced at 1 m (Fig. 6.B). Temperature recorded in the middle of the lagoon at 22 m depth at the B2 station followed the same general trend, with a delayed response and smoother daily variability, indicating greater thermal inertia of deep lagoon waters. Overall, during this unprecedented event, the lagoon alternated between high-level and *ranoa* phases, and winds were blowing mostly from E/SE. Unexpectedly, oceanic (exacerbated ocean-lagoon exchanges during certain periods such as the end of February 2024) and wind forcings seemed to have only “marginally” affected the high temperature trends suggesting that exceptionally strong solar fluxes, likely associated with anomalously warm air temperatures, were the primary contributing factors.

https://doi.org/10.5194/essd-2025-692
Preprint. Discussion started: 27 November 2025

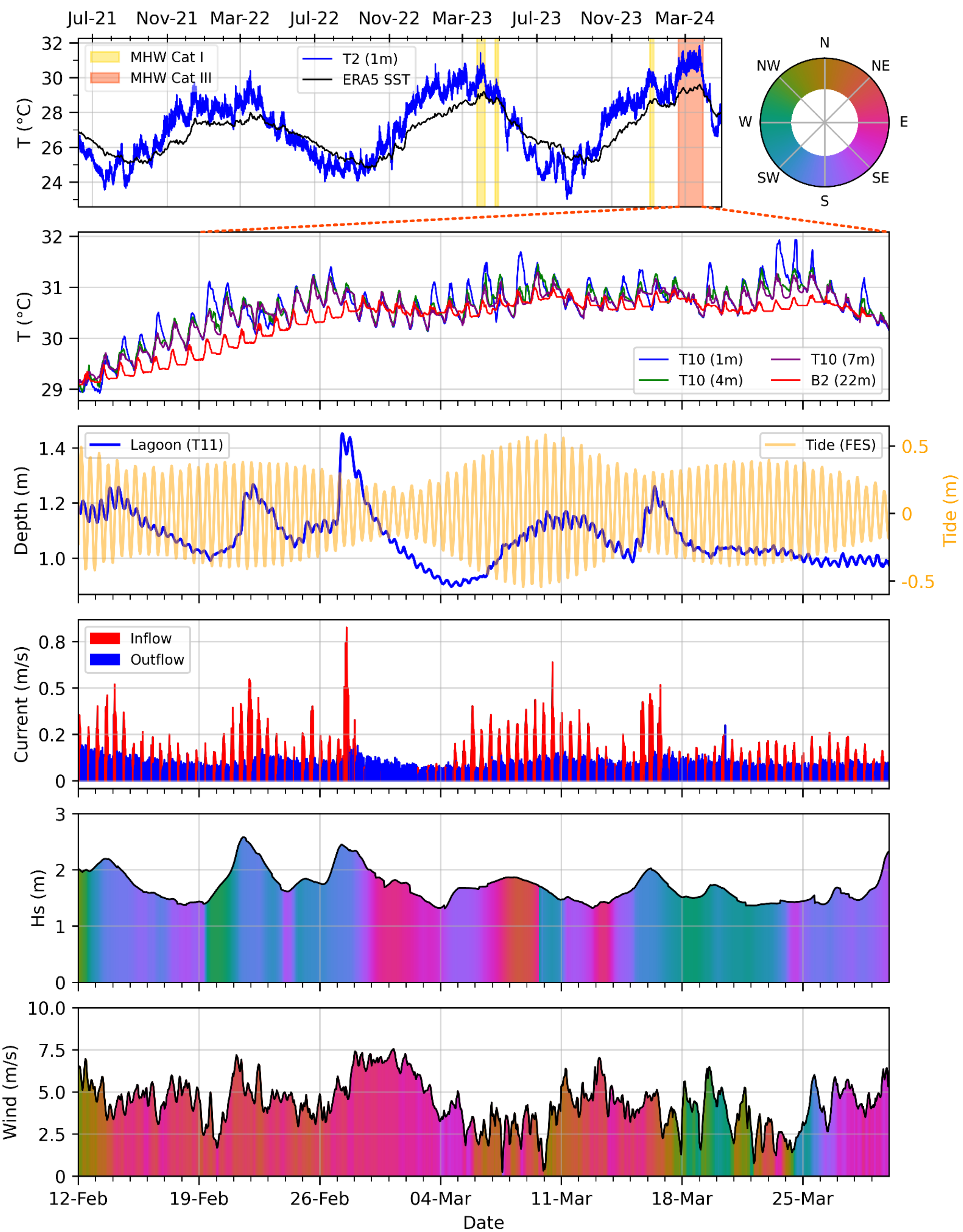

326

https://doi.org/10.5194/essd-2025-692
Preprint. Discussion started: 27 November 2025

Figure 6: From top to bottom: (A) Temperature interannual time series at T2 station (blue) and ERA5 SST at 18.5°S, 136.5°W (black). Marine heatwave categories were computed from a statistical hindcast model (Van Wynsberge et al., in revision). (B) Zoom on the 2024 MHW category III event at T10 (1 m, 4 m, 7 m) and ADCP B2 station. (C) Oceanic tide (recomposed from FES2012 global tide solution at 18.75°S, 136.6°W) and lagoon level at T11. (D) Current speed in hoa at A1. (E) Significant wave height and wave direction extracted from ERA5 at 18.75°S, 136.6°W. (F) Wind speed and direction computed from wind components extracted from ERA5 at 18.5°S, 136.5°W.

Figure 7 displays CTD profiles at two different sampling dates (17 October 2023 and 29 March 2024). Globally, CTD network evidenced a southeast-northwest gradient across the three basins, the northwest basins showing warmer and more saline waters. Toward the southeastern part of the lagoon, temperature and salinity decrease at both dates. CTD profiles network (that did not cover the southeast part of the lagoon) captured on the 17 October 2023 shows quite marked stratification in the Northwest basin, but also reflects the influence of hoa in the central part of the lagoon, mainly visible through salinity, with variations of nearly 0.6 PSU between surface and bottom values. During the 2024 MHW event (29 March 2024), water columns displayed limited stratification in terms of temperature. Lowest temperatures were found at immediate proximity of ho (e.g M40, M15, Fig. 3.B) in the intermediate basin.

https://doi.org/10.5194/essd-2025-692
Preprint. Discussion started: 27 November 2025

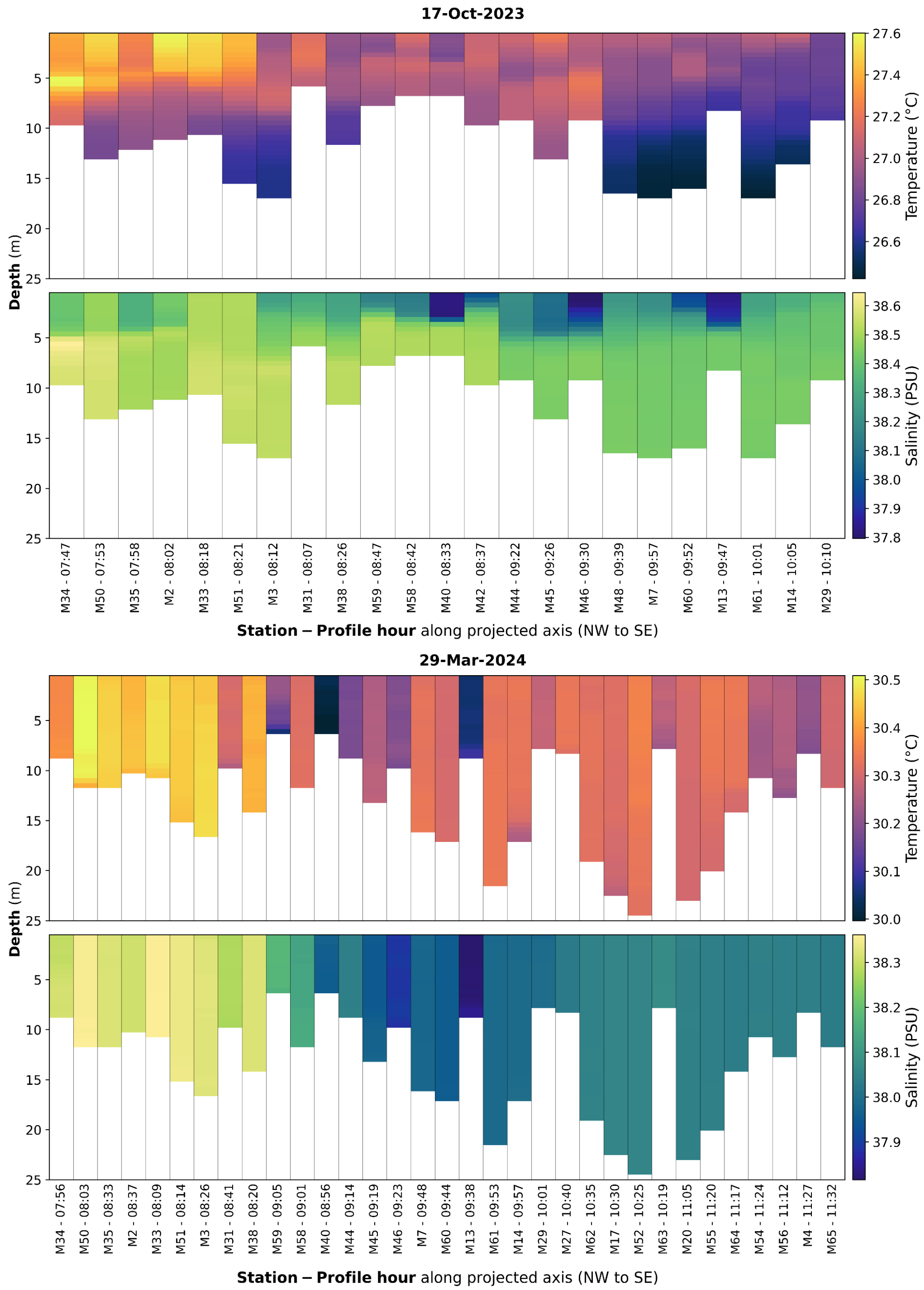

Figure 7: Temperature and salinity profiles for stations projected along Reao's main axis. Profiles are arranged from northwest (left) to southeast (right) across the atoll lagoon. Top : CTD profiles on 17 October 2023.. Bottom: CTD Profiles during the 2024 MHW event on 29 March 2024.

https://doi.org/10.5194/essd-2025-692
Preprint. Discussion started: 27 November 2025

7. Data Availability

The whole dataset presented herein is publicly available in NetCDF format through the SEANOE open data platform (https://www.seanoe.org/, Seanoe, 2023) in a dedicated repository. DOI: https://doi.org/10.17882/105885 (Le Gendre et al., 2025a).

8. Conclusions

Our dataset presented for the lagoon of Reao Atoll provides a unique and comprehensive record of thermal fluctuations and hydrodynamics in a semi-closed tropical ecosystem, including an exceptional MHW event in summer 2024. Multi-year and multi-depth observations will allow for a detailed characterization of the spatial and vertical variability of temperature, ocean-lagoon exchanges through the *hoa*, internal circulation, and lagoon water level dynamics. Beyond improving our understanding of the functioning of semi-closed atolls and their vulnerability to thermal stress, these data will provide valuable support for future modeling (e..g statistical or hydrodynamics) and remote sensing analyses. The availability of the data in a standardized NetCDF format, along with comprehensive metadata, facilitates reuse for future works.

Author contributions. SVW set up the ANR GAIA project and raised funds. RLG and SVW designed and conducted the experiments as principal investigators. EL and CC organized, processed, checked, and archived the data sets. EL prepared the initial version of the paper and designed the figures, with contributions from all co-authors.

Competing interests. The contact author has declared that none of the authors has any competing interests.

Acknowledgements. This work was supported by the Agence National de la Recherche [ANR-21-CE32-0011-01 GAIA] and the Direction des Ressources Marine (DRM). We thank Pahuatini Michel, Liao Vetea, Maamaatuaiahutapu Moana, Moeroa Matangi, Remoissenet Georges, Richmond Teriipaia, and Varillon David for their assistance with logger maintenance, and the mayor of Reao Mr M. Lenoir for giving us permission to deploy the instruments in the lagoon. We also extend our gratitude to Serge Andréfouët and Oriane Bruyère for their advice that helped design the sampling strategy and for providing the map of French Polynesia.

Financial support. This research has been supported entirely by the *Agence National de la Recherche* [ANR-21-CE32-0011-01 GAIA] and the *Direction des Ressources Marines* (DRM) of French Polynesia.

References

Amrari, S., Bourassin, E., Andréfouët, S., Soulard, B., Lemonnier, H., and Le Gendre, R.: Shallow Water Bathymetry Retrieval Using a Band-Optimization Iterative Approach: Application to New Caledonia Coral Reef Lagoons Using Sentinel-2 Data, Remote Sensing, 13, 4108, https://doi.org/10.3390/rs13204108, 2021.

Andréfouët, S. and Paul, M.: Atolls of the world: A reappraisal from an optical remote sensing and global mapping perspective, Marine Pollution Bulletin, 194, 115400, https://doi.org/10.1016/j.marpolbul.2023.115400, 2023.

Andréfouët, S., Desclaux, T., Buttin, J., Jullien, S., Aucan, J., Le Gendre, R., and Liao, V.: Periodicity of wave-driven flows and lagoon water renewal for 74 Central Pacific Ocean atolls, Marine Pollution Bulletin, 179, 113748, https://doi.org/10.1016/j.marpolbul.2022.113748, 2022.

Andréfouët, S., Bruyère, O., Liao, V., and Le Gendre, R.: Hydrodynamical impact of the July 2022 'Code Red' distant mega-swell on Apataki Atoll, Tuamotu Archipelago, Global and Planetary Change, 228, 104194, https://doi.org/10.1016/j.gloplacha.2023.104194, 2023.

Andréfouët, S., Van Wynsberge, S., and Remoissenet, G.: A typology of giant clam shell deposits in eastern Tuamotu-Gambier atolls (French Polynesia) to guide conservation and exploitation measures, Regional Studies in Marine Science, 89, 104364, https://doi.org/10.1016/j.rsma.2025.104364, 2025.

Aucan, J., Desclaux, T., Le Gendre, R., Liao, V., and Andréfouët, S.: Tide and wave driven flow across the rim reef of the atoll of Raroia (Tuamotu, French Polynesia), Marine Pollution Bulletin, 171, 112718, https://doi.org/10.1016/j.marpolbul.2021.112718, 2021.

Bruyère, O., Soulard, B., Lemonnier, H., Laugier, T., Hubert, M., Petton, S., Desclaux, T., Van Wynsberge, S., Le Tesson, E., Lefèvre, J., Dumas, F., Kayara, J.-F., Bourassin, E., Lalau, N., Antypas, F., and Le Gendre, R.: Hydrodynamic and hydrological processes within a variety of coral reef lagoons: field observations during six cyclonic seasons in New Caledonia, Earth System Science Data, 14, 5439–5462, https://doi.org/10.5194/essd-14-5439-2022, 2022.

Bruyère, O., Le Gendre, R., Chauveau, M., Bourgeois, B., Varillon, D., Butscher, J., Trophime, T., Follin, Y., Aucan, J., Liao, V., and Andréfouët, S.: Lagoon hydrodynamics of pearl farming atolls: the case of Raroia, Takapoto, Apataki and Takaroa (French Polynesia), Earth System Science Data, 15, 5553–5573, https://doi.org/10.5194/essd-15-5553-2023, 2023.

Bruyère, O., Le Gendre, R., Liao, V., and Andréfouët, S.: Lagoon hydrodynamics of pearl farming islands: the case of Gambier (French Polynesia), Earth System Science Data, 16, 667–679, https://doi.org/10.5194/essd-16-667-2024, 2024.

Dumas, F., Le Gendre, R., Thomas, Y., and Andréfouët, S.: Tidal flushing and wind driven circulation of Ahe atoll lagoon (Tuamotu Archipelago, French Polynesia) from *in situ* observations and numerical modelling, Marine Pollution Bulletin, 65, 425–440, https://doi.org/10.1016/j.marpolbul.2012.05.041, 2012.

Dutheil, C., Andrefouët, S., Jullien, S., Le Gendre, R., Aucan, J., and Menkes, C.: Characterization of south central Pacific Ocean wind regimes in present and future climate for pearl farming application, Marine Pollution Bulletin, 160, 111584, https://doi.org/10.1016/j.marpolbul.2020.111584, 2020.

https://doi.org/10.5194/essd-2025-692
Preprint. Discussion started: 27 November 2025

Dutheil, C., Jullien, S., Aucan, J., Menkes, C., Le Gendre, R., and Andréfouët, S.: The wave regimes of the Central Pacific Ocean with a focus on pearl farming atolls, Marine Pollution Bulletin, 162, 111751, https://doi.org/10.1016/j.marpolbul.2020.111751, 2021.

Gilbert, A., Yan, L., Remoissenet, G., Andréfouët, S., Payri, C., and Chancerelle, Y.: Extraordinarily high giant clam density under protection in Tatakoto atoll (Eastern Tuamotu archipelago, French Polynesia), Coral Reefs, 24, 495–495, https://doi.org/10.1007/s00338-005-0494-2, 2005.

Le Gendre, R., Ladet, E., Chevillard, C., Trophime, T., Bruyere, O., and Van Wynsberge, S.: Lagoon temperature and hydrodynamics of Reao atoll (Tuamotu Archipelago), https://doi.org/10.17882/105885, 2025a.

Le Gendre, R., Varillon, D., Fiat, S., Hocdé, R., de Ramon N'Yeurt, A., Andréfouët, S., Aucan, J., Cravatte, S., Duphil, M., Ganachaud, A., Gaudron, B., Kestenare, E., Liao, V., Pelletier, B., Peltier, A., Schaefer, A.-L., Trophime, T., Van Wynsberge, S., Dandonneau, Y., Allenbach, M., and Menkes, C.: ReefTEMPS: the Pacific Islands coastal temperature network, Earth System Science Data, 17, 5277–5301, https://doi.org/10.5194/essd-17-5277-2025, 2025b.

McCabe, R. M., Estrade, P., Middleton, J. H., Melville, W. K., Roughan, M., and Lenain, L.: Temperature variability in a shallow, tidally isolated coral reef lagoon, Journal of Geophysical Research: Oceans, 115, https://doi.org/10.1029/2009JC006023, 2010.

Mies, M., Dor, P., Güth, A. Z., and Sumida, P. Y. G.: Production in Giant Clam Aquaculture: Trends and Challenges, Reviews in Fisheries Science & Aquaculture, 25, 286–296, https://doi.org/10.1080/23308249.2017.1285864, 2017.

Neo, M. L., Eckman, W., Vicentuan, K., Teo, S. L.-M., and Todd, P. A.: The ecological significance of giant clams in coral reef ecosystems, Biological Conservation, 181, 111–123, https://doi.org/10.1016/j.biocon.2014.11.004, 2015.

Pagli, B., Izumo, T., Barboni, A., Chevillard, C., Dutheil, C., Legrand, R., Menkes, C., Rocuet, C., and Cravatte, S.: Marine Heatwaves across the central South Pacific: characteristics, mechanisms, and modulation by the El Niño Southern Oscillation, EGUsphere, 1–35, https://doi.org/10.5194/egusphere-2025-4166, 2025.

Pirazzoli, A., Delibrias, G., Montaggioni, L. F., Saliège, J. F., and Vergnaud-Grazzini, C.: Vitesse de croissance latérale des platiers et évolutions morphologiques récentes de l'atoll de de Reao, Iles Tuamotu, Polynésie Française, Annales de l'Institut Océanographique, 63, 57–68, 1987.

Quéré, R., Friot, C., Van Wynsberge, S., and Le Gendre, R.: Bathymetry of the lagoon and hoa of Reao, Tuamotu Archipelago, https://doi.org/10.17882/108293, 2025.

Quere, R., Van Wynsberge, S., and Le Gendre, R.: Optimisation d'une bathymétrie dérivée satellite pour le lagon de Reao, Tuamotu, 2025.

Rougerie, F.: Nature et fonctionnement des atolls des Tuamotu (Polynésie Française), Oceanologica Acta, 18, 61–78, 1995.

Storlazzi, C. D., Gingerich, S. B., van Dongeren, A., Cheriton, O. M., Swarzenski, P. W., Quataert, E., Voss, C. I., Field, D. W., Annamalai, H., Piniak, G. A., and McCall, R.: Most atolls will be uninhabitable by the mid-21st century because of sea-level rise exacerbating wave-driven flooding, Science Advances, 4, eaap9741, https://doi.org/10.1126/sciadv.aap9741, 2018.

Teaniniuraitemoana, V., Monaco, C. J., Célariès, M., Jauffrais, T., and Van Wynsberge, S.: Light intensity modulates the effect of thermal stress on giant clams and their symbiotic zooxanthellae, Coral Reefs, 44, 1449–1465, https://doi.org/10.1007/s00338-025-02708-8, 2025.

Van Wynsberge, S. and Andréfouët, S.: The Future of Giant Clam-Dominated Lagoon Ecosystems Facing Climate Change, Curr Clim Change Rep, 3, 261–270, https://doi.org/10.1007/s40641-017-0078-6, 2017.

Van Wynsberge, S., Andréfouët, S., Gaertner-Mazouni, N., Wabnitz, C. C. C., Gilbert, A., Remoissenet, G., Payri, C., and Fauvelot, C.: Drivers of density for the exploited giant clam Tridacna maxima: a meta-analysis, Fish and Fisheries, 17, 567–584, https://doi.org/10.1111/faf.12127, 2016.

Van Wynsberge, S., Menkes, C., Le Gendre, R., Passfield, T., and Andréfouët, S.: Are Sea Surface Temperature satellite measurements reliable proxies of lagoon temperature in the South Pacific?, Estuarine, Coastal and Shelf Science, 199, 117–124, https://doi.org/10.1016/j.ecss.2017.09.033, 2017.

Van Wynsberge, S., Quéré, R., Andréfouët, S., Autret, E., and Le Gendre, R.: Spatial variability of temperature inside atoll lagoons assessed with Landsat-8 satellite imagery, Remote Sensing Applications: Society and Environment, 36, 101340, https://doi.org/10.1016/j.rsase.2024.101340, 2024.

Wynsberge, S. V.: Approche comparée, intégrée et spatialisée pour la gestion d'une ressource emblématique exploitée en Polynésie française et Nouvelle-Calédonie le cas du bénitier Tridacna maxima : le cas du bénitier (Tridacna maxima), thesis, Polynésie française, 2016.

Appendix A

Table A1. Detailed list of instruments moored at the Reao lagoon.

Station	Instrument	Raw parameters	Date Start (UTC)	Date End (UTC)	Longitude (deg W)	Latitude (deg S)	Freq	Depth (m)	Processed parameters	Legs
A1	AQUADOPP	Current, pressure, temperature	2023-10-13 22:00:00	2024-03-30 00:40:00	-136.389478	-18.51418	20 minutes	1.45	Current speed and direction, temperature, water level	5
A2	AQUADOPP	Current, pressure, temperature	2023-10-13 22:00:00	2024-03-30 00:00:00	-136.360166	-18.543549	20 minutes	1.77	Current speed and direction, temperature, water level	5

https://doi.org/10.5194/essd-2025-692
Preprint. Discussion started: 27 November 2025

ADCP_B1	ADCP	Current, pressure, temperature	2023-10-14 19:40:00	2024-03-08 11:00:00	-136.442767	-18.474505	20 minutes	17.54	Current speed and direction, temperature, water level	5
ADCP_B2	ADCP	Current, pressure, temperature	2023-10-14 01:00:00	2024-03-29 08:40:00	-136.385366	-18.505844	20 minutes	21.71	Current speed and direction, temperature, water level	5
ADCP_B3	ADCP	Current, pressure, temperature	2023-10-14 01:00:00	2023-12-05 00:00:00	-136.318634	-18.558222	20 minutes	22.92	Current speed and direction, temperature, water level	5
CTD	SBE19 Plus	Conductivity, temperature, depth	2023-06-02 19:01:00	2024-03-29 21:32:00	X	X	4 Hz	X	Conductivity, Temperature, Depth	4, 5
L1	LOWELL	Inclination, temperature	2023-06-06 10:00:00	2023-08-11 09:59:00	-136.389495	-18.514144	1 minute	1.6	Current speed and direction, temperature, water level	4
L2	LOWELL	Inclination, temperature	2023-06-06 10:00:00	2024-01-17 09:59:00	-136.42875	-18.485563	1 minute	2.0	Current speed and direction, temperature, water level	4, 5
L3	LOWELL	Inclination, temperature	2023-06-06 10:00:00	2024-01-17 09:59:00	-136.389495	-18.514144	1 minute	1.6	Current speed and direction, temperature, water level	4, 5
L4	LOWELL	Inclination, temperature	2023-06-06 10:00:00	2024-01-17 09:59:00	-136.42875	-18.485563	1 minute	2.0	Current speed and direction, temperature, water level	4, 5
L5	LOWELL	Inclination, temperature	2023-06-06 10:00:00	2024-01-17 09:59:00	-136.42875	-18.485563	1 minute	2.0	Current speed and direction, temperature, water level	4, 5

https://doi.org/10.5194/essd-2025-692
Preprint. Discussion started: 27 November 2025

T1	TWR2050	Pressure, temperature	2016-12-17 00:00:00	2017-06-29 03:30:00	-136.411855	-18.494014	30 minutes	3.6	Temperature, water level	1
T2	SBE56	Temperature	2021-06-08 10:01:25	2025-04-28 09:49:03	-136.424779	-18.483047	20 minutes	1.25	Temperature	2, 3, 4, 5, 6
T3	RBRduet	Pressure, temperature	2022-04-29 10:13:29	2022-05-06 09:58:29	-136.435944	-18.472807	15 minutes	1.7	Temperature, water level	3
T4_2m	SBE56	Temperature	2022-04-30 10:00:00	2024-03-30 09:56:02	-136.3330652994	-18.5655256421	30 minutes	1.72	Temperature	3, 4, 5
T4_4m	SBE56	Temperature	2023-10-16 10:21:50	2024-03-29 09:51:50	-136.3329796838	-18.5654973138	30 minutes	4.5	Temperature	5
T4_7m	SBE56	Temperature	2023-10-16 10:27:23	2024-03-29 09:57:23	-136.3328795619	-18.5654819472	30 minutes	7.0	Temperature	5
T5	SBE56	Temperature	2022-04-30 10:00:00	2023-10-13 09:56:07	-136.342201	-18.54318	30 minutes	1.8	Temperature	3, 4
T6	SBE56	Temperature	2022-04-30 10:00:00	2024-04-01 09:50:25	-136.356377	-18.521482	30 minutes	1.25	Temperature	3, 4, 5
T7	SBE56	Temperature	2022-04-30 10:00:00	2023-10-13 09:42:32	-136.390002	-18.513607	30 minutes	1.15	Temperature	3, 4

https://doi.org/10.5194/essd-2025-692
Preprint. Discussion started: 27 November 2025

T8	SBE56	Temperature	2022-04-30 10:00:00	2023-10-13 09:53:42	-136.376241	-18.50116	30 minutes	1.4	Temperature	3, 4
T9	SBE56	Temperature	2022-04-30 10:00:00	2023-10-13 09:41:03	-136.396765	-18.497568	30 minutes	1.4	Temperature	3, 4
T10_1m	SBE56	Temperature	2022-05-04 10:29:59	2024-03-31 09:55:22	-136.442570405	-18.48093 29083	30 minutes	1.15	Temperature	3, 4, 5
T10_4m	SBE56	Temperature	2023-10-15 10:23:08	2024-03-31 09:53:08	-136.4425084927	-18.4808935738	30 minutes	4.5	Temperature	5
T10_7m	SBE56	Temperature	2023-10-15 10:25:07	2024-03-31 09:55:07	-136.4424286355	-18.4807671817	30 minutes	7.0	Temperature	5
T11	RBRduet	Pressure, temperature	2022-05-08 10:05:56	2024-04-01 17:29:00	-136.435903	-18.472794	15 minutes	1.0238	Temperature, water level	3, 4, 5

https://doi.org/10.5194/essd-2025-692
Preprint. Discussion started: 27 November 2025

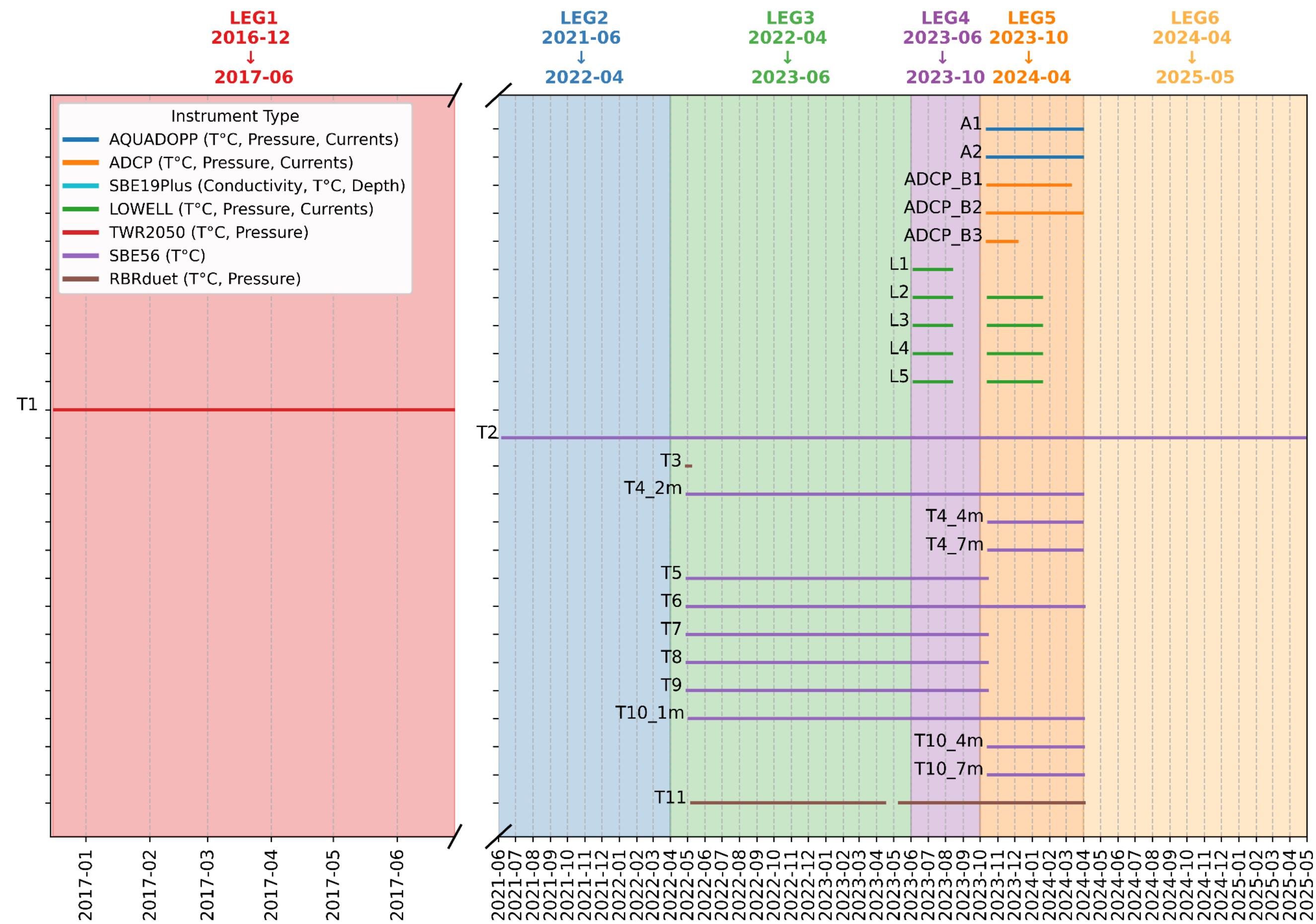

Figure A1: Instrument deployments at Reao Atoll, including the first deployment (December 2016 to June 2017) and subsequent deployments conducted under the GAIA project (June 2021 to May 2025).

Figure A2: Zooms on the locations of the five instrumented *hoa* (© Google Maps)